

COMPASS-U Global Heat Balance Calculations

Han Zhang¹, Member, IEEE, Peter Titus¹, Matej Peterka, Petr Barton¹, and Petr Vondracek¹

Abstract—COMPASS-U is a medium size, high magnetic field experimental tokamak ($R = 0.9$ m, $B_t = 5$ T, and $I_p = 2$ MA), built at the Institute of Plasma Physics, Czech Academy of Sciences (IPP-CAS). This global heat balance calculation for COMPASS-U was done at Princeton Plasma Physics Laboratory (PPPL). Based on our previous experience of building global thermal model for National Spherical Torus Experiment-Upgrade (NSTX-U) at PPPL, this 2-D global thermal model geometry represents a typical cross section of COMPASS-U machine. The model includes thermal radiation, conduction, and convection among components and also between the machine and outer environment. Helium gas heating/cooling was modeled with fluid element and surface element. This model was used to calculate component temperatures and heat distribution during heat up, cryogenic cool down, normal operation, and fault operation scenarios. Definition of 14 main thermal scenarios was provided by IPP-CAS. First nine are normal operation scenarios. Scenarios #10–#14 are fault scenarios. Some results of thermal scenario #5 will be given and discussed in this article, including peak temperatures, temperature ratcheting, energy distribution, and required cooling power.

Index Terms—Ansys, COMPASS-U, global thermal analysis, heat balance.

I. INTRODUCTION

COMPASS-U is a medium size, high magnetic field experimental tokamak ($R = 0.9$ m, $B_t \geq 5$ T, and $I_p = 2$ MA), built at the Institute of Plasma Physics, Czech Academy of Sciences (IPP-CAS). This tokamak is expected to operate at high magnetic field and $P_{sep}B_t/(qAR)$ ratio, which will support ITER operation research and benefit to solve key issues for DEMO construction, e.g., divertor physics including plasma exhaust with extreme heat fluxes and advanced confinement modes [1].

Although computing technologies have advanced more recently, e.g., parallel computing, distributed computing, and cloud computing, simulating a complicated large machine with all the components and features is still costly, time-consuming,

Manuscript received 31 January 2022; revised 5 August 2022; accepted 21 September 2022. Date of publication 30 December 2022; date of current version 24 March 2023. This work was supported by U.S. Department of Energy (DOE) Contract No. DE-AC02-09CH11466 and has been carried out within the framework of the project COMPASS-U: Tokamak for cutting-edge fusion research No. CZ.02.1.01/0.0/0.0/16_019/0000768 and co-funded from European structural and investment funds. The review of this article was arranged by Senior Editor G. H. Neilson. (Corresponding author: Han Zhang.)

Han Zhang and Peter Titus are with the Princeton Plasma Physics Laboratory, Princeton, NJ 08540 USA (e-mail: hzhang@pppl.gov; ptitus@pppl.gov).

Matej Peterka and Petr Barton are with the Institute of Plasma Physics of the Czech Academy of Sciences, 182 00 Prague, Czech Republic, and also with the Faculty of Mathematics and Physics, Charles University, 12116 Prague, Czech Republic (e-mail: peterka@ipp.cas.cz; barton@ipp.cas.cz).

Petr Vondracek is with the Institute of Plasma Physics of the Czech Academy of Sciences, 182 00 Prague, Czech Republic (e-mail: vondracek@ipp.cas.cz).

Color versions of one or more figures in this article are available at <https://doi.org/10.1109/TPS.2022.3225719>.

Digital Object Identifier 10.1109/TPS.2022.3225719

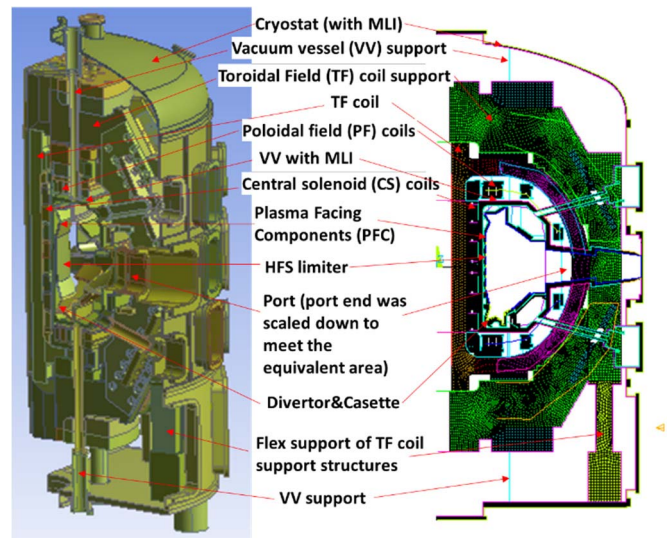


Fig. 1. 2-D global thermal model for COMPASS-U.

and software-intensive. Instead, global-submodeling provides a feasible and flexible way to efficiently simulate the overall to detailed behaviors of a complicated machine, like fusion tokamak. It is possible to use coarse mesh in the global model with more mathematical and physical representations, as the local features of the submodel do not have any dominant impact on the overall response of the system. We then define a refined submodel without small changes and apply thermal, electromagnetic, or structural boundary conditions mapped from global model to study critical region without solving for the whole model. For National Spherical Torus Experiment-Upgrade (NSTX-U) recovery, the global structural model described in [2] was built to study overall load, deformations, and stress, and displacement result was then mapped to sub-poloidal field (PF) coil model for further evaluation of coil stress. Another global thermal model described in [3] was to calculate radiation heat transfer in DEMO. The first complete global thermal model was developed for NSTX-U recovery, which includes all the dominant components, radiation, conduction, convection and thermal contact, water, and gas heating and cooling, to compute global temperature distribution and heat flow in both steady-state and transient processes [4]. This technique was then used in COMPASS-U to build this global thermal model.

This global heat balance calculation was done at Princeton Plasma Physics Laboratory (PPPL). The 2-D model geometry was mainly extracted from a typical cross section of COMPASS-U machine but modifying and adding the mathematical 2-D representations of discontinuous components and features (Fig. 1). For any components that will not influence global thermal effect, they can be neglected in the global model and only considered in submodels with correct

boundary conditions, e.g., mapped temperatures or applied heat flux. This model includes thermal radiation, conduction, and convection among components and between the machine and outer environment. Helium gas heating/cooling was modeled with fluid element and surface element. Convection between cryostat and outer environment is also modeled.

This model was used to calculate component temperatures distribution and heat flow during heat up, cryogenic cool down, normal operation, and fault operation scenarios, both transient and steady state. For example, plasma heat load can be applied to calculate transient temperature ratcheting. Steady state can be run to compare different bake-out, heat up, or cooling schemes. Joule heat load from electromagnetic analysis of coil current or eddy current can also be applied to coils or other components. The temperature profile can be mapped to 3-D submodels or provide boundary conditions for other structural model analysis. The thermal model can also be converted to 2-D structural model to estimate thermal expansion and stresses. A 2-D model will significantly reduce computation and thus be able to run simulations that require large computations, such as long-time transient process like ratcheting and overnight cooling.

II. MODEL DESCRIPTION

Inside the cryostat is the vacuum environment, and thus, only conduction and radiation heat transfer will take effect. Several radiation loops were built to calculate radiation heat transfer: among plasma facing components (PFCs), from PFC support structures to vacuum vessel (VV), from VV to coils and coil support structures, and from VV to cryostat and from cryostat to outer environment. It is known that 2-D model internally assumes that everything is toroidally continuous. To mathematically represent a 3-D machine in a 2-D model, we need to deal with equivalent radiation and conduction for both steady state and transient thermal simulation, and thermal mass needs to be scaled, which only takes effect in transient process.

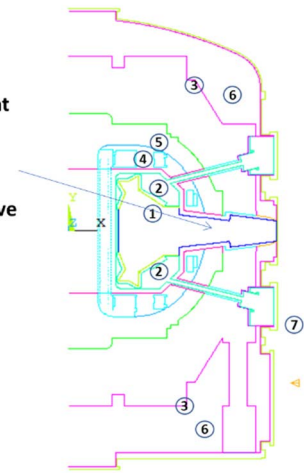
For thermal radiation, separate radiation loops were built between components that can “see” each other to form an enclosure. Fig. 2 shows and lists radiation enclosures and emissivity settings. For components with toroidally discontinuous surface, form factors were calculated using a separate model (Fig. 3) and then scaled the emissivity in the global thermal model by view factor from high-temperature component to low-temperature one, so that total radiation heat will be the same as 3-D machine. In ANSYS, standard radiation equation is solved iteratively and restricted to gray-diffuse surfaces. Diffuse means that emissivity and absorptivity do not depend on direction. Although multilayer insulation (MLI) surface is normally shining and mirror-like, MLI typically is wrapped with an uneven surface, and thus, we think that this diffusion assumption is reasonable

$$Q = \sigma \varepsilon F A (T_i^4 - T_j^4)$$

where

- Q = heat flow rate between nodes I and J ;
- σ = Stefan–Boltzmann’s constant;

Machine design uses straight port extension which has same area for both ends. In the global model, port dimension is adjusted to have same area for this toroidal continuous port as discrete ports of real machine.



Radiation loops:

1. PFC, HFS, horizontal port: emis=0.17 (tungston) 0.28 (inconel)
2. Between PFC supt and VV inside emis=0.28 (inconel)
3. From VV MLI outside to cryostat: emis=0.04*0.199 (MLI)
4. From VV MLI outside to TF emis=0.04*0.276 (MLI)
5. From VV MLI outside to TF support emis=0.04*0.796 (MLI)
6. From cryostat MLI to TF support emis=0.04*0.868 (MLI)
7. Outside cryostat, emis=0.26 (ss)

Fig. 2. Radiation loops in the model with emissivity setting.

Top view of VV, TF, TF supt and cryostat

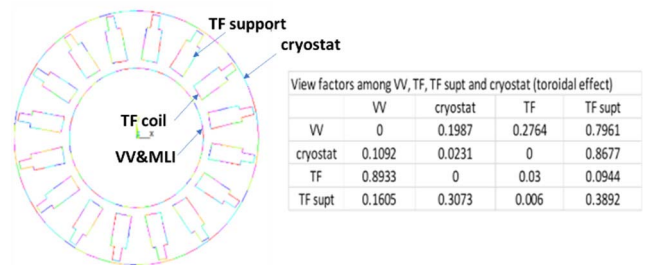


Fig. 3. View factor calculation for VV (with MLI outside), TF coil, TF support structures, and cryostat (with MLI inside). Note that TF coils and TF support structures have some overlap.

ε = emissivity;

F = geometric form factor;

A = area of element;

T_i and T_j = absolute temperatures at nodes I and J .

Using the radiation from VV MLI to cryostat as an example, in the 2-D global model, $Q_{vv \rightarrow cryostat} = \sigma \varepsilon F_{VV \rightarrow cryostat} A_{VV} (T_{VV}^4 - T_{cryostat}^4)$ and $F_{VV \rightarrow cryostat} = 1$. In the 3-D machine, form factor of VV \rightarrow cryostat is 0.199 (Fig. 3), we cannot scale form factor in 2-D model, instead emissivity is scaled, so that the radiation heat from VV \rightarrow cryostat will be the same as 3-D machine.

The thermal conduction of toroidally discontinuous parts, we can either use solid elements with anisotropic or scaled material properties or represent with link elements of equivalent conduction area. Fig. 4 shows some examples. Fig. 4(a) shows the solid element with scaled mass and thermal conductivity to represent cassette sections with cut-outs. Fig. 4(b) shows that the support of High-field-side (HFS) limiter is modeled with link element with equivalent length and

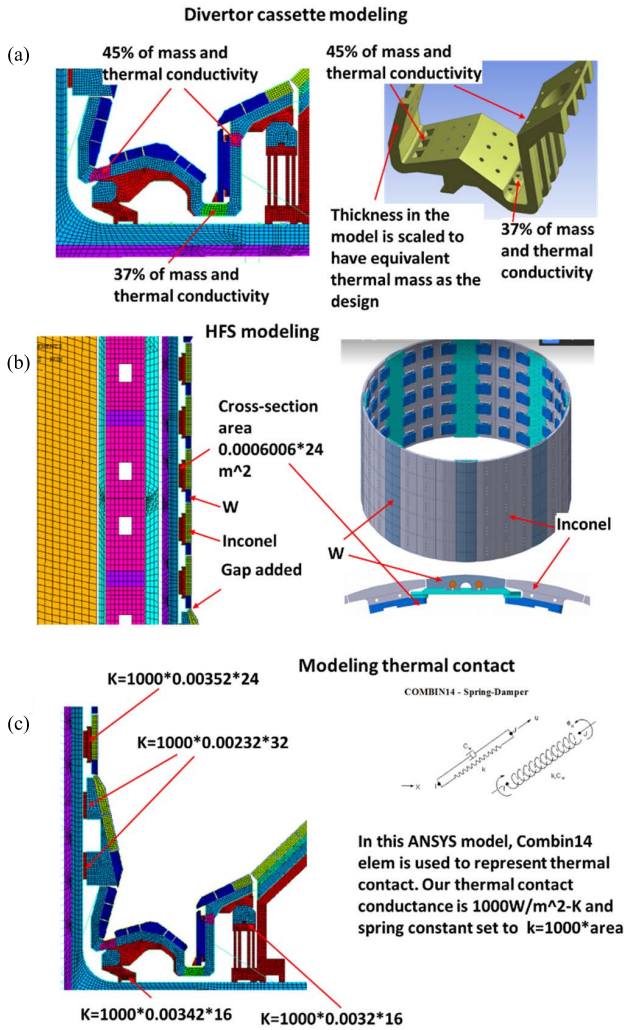


Fig. 4. Examples in this global model to show some 2-D representation of toroidal discontinuous parts. (a) Density, thermal conductivity, and thickness etc., were scaled to represent the cut-out or thickness variance of divertor cassette. (b) HFS limiter is modeled with link element of equivalent length and cross-section area. Toroidally alternating material of HFS limiter (tungsten and Inconel) was modeled in poloidal direction with equivalent thermal mass. (c) Modeling thermal contact with combin14 element in ANSYS and setting of the spring constant.

cross-sectional area. To represent the alternating material of HFS limiter toroidally between tungsten and Inconel, poloidally alternated materials with equivalent thermal mass are built in the model to address the different material behavior. Equivalent thermal mass will only take effect in transient analysis, which can be done by scaling either the density or specific heat. Fig. 4(c) shows the modeling of thermal contact with combin14 element in ANSYS and setting of the spring constant.

Fig. 5 shows the helium gas heating/cooling modeling. Coolants were modeled with fluid element in ANSYS (fluid 116). Cooling channels were modeled with surface convection elements and corresponding heat transfer coefficients. Modeling exact 3-D coolant flow is not possible. Instead, in this 2-D model, some surface elements (surf151 elem) were uniformly distributed along the cooling path with total area equal to the fluid–solid interface area of the corresponding cooling line. A 2-D fluid flow path was created along the cooling surface with equivalent flow rate. The heat transfer

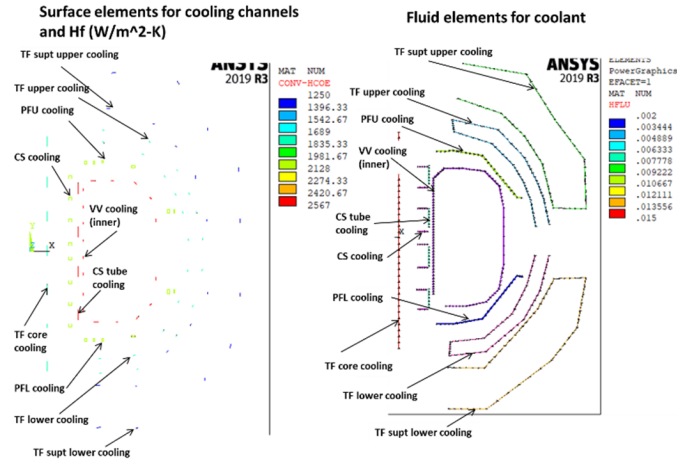
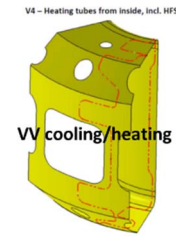


Fig. 5. Fluid heating/cooling in this model.



1. ID: area: $3.14 \times 0.016/2 \times 1.5 \times 16 = 0.6 \text{ m}^2$ (1.5m long, totally 16 cooling lines)
2. Top, bottom and OD: area: $3.14 \times 0.016/2 \times (6.3-1.5) \times 16 = 1.93 \text{ m}^2$ (4.8m long, and 16 cooling lines)
3. heating: $\text{Hf}=2509 \text{ W/m}^2\text{-K}$ (helium gas, 60 bar, $500 \text{ }^\circ\text{C}$, viscosity $\mu=3.86\text{E-}5 \text{ Pa}\cdot\text{s}$, $k=0.304 \text{ W/m}\cdot\text{K}$, $\text{Re}=41401$, $\text{Pr}=0.66$, $\text{Nu}=99$, $\rho=3.7021 \text{ kg/m}^3$, flow rate 0.01507 kg/s)
4. 500°C heating: $\text{Hf}=2509 \text{ W/m}^2\text{-K}$ (helium gas, 60 bar, $500 \text{ }^\circ\text{C}$, viscosity $\mu=3.86\text{E-}5 \text{ Pa}\cdot\text{s}$, $k=0.304 \text{ W/m}\cdot\text{K}$, $\text{Re}=41401$, $\text{Pr}=0.66$, $\text{Nu}=99$, $\rho=3.7021 \text{ kg/m}^3$, flow rate 0.01507 kg/s)
5. Room temperature cooling: $\text{Hf}=2125 \text{ W/m}^2\text{-K}$ (helium gas, 60 bar, $27 \text{ }^\circ\text{C}$, viscosity $\mu=1.99\text{E-}5 \text{ Pa}\cdot\text{s}$, $k=0.157 \text{ W/m}\cdot\text{K}$, $\text{Re}=79947$, $\text{Pr}=0.66$, $\text{Nu}=162.9$, $\rho=9.362 \text{ kg/m}^3$, flow rate 0.01507 kg/s)

Fig. 6. Calculating the parameters of helium gas heating/cooling of VV.

coefficient between the bulk of the fluid and the pipe surface of an internal turbulent flow can be expressed explicitly as

$$h = \text{Nu} \cdot k/D \quad (1)$$

where

- Nu Nusselt number: $\text{Nu} = 0.023 \text{Re}^{0.8} \text{Pr}^n$;
- n 0.4 for heating (wall hotter than the bulk fluid) and 0.33 for cooling (wall cooler than the bulk fluid);
- k thermal conductivity of fluid;
- D hydraulic diameter.

Fig. 6 shows an example of calculating cooling line parameters, which were used to build fluid flow and interface element in the global model. This way will give result of average cooling effect along the surface but cannot address the detailed spatial temperature fluctuation due to cooling.

III. SOME THERMAL RESULTS

Table I lists the thermal scenarios defined by the COMPASS-U group (IPP-CAS). Some are done and some are still ongoing. Among them, scenarios 1–9 are normal operations and scenarios 10–14 are fault operations.

According to the operating scenarios provided, during a full shot, 10 MJ is deposited from plasma to the outer vertical target (OVT), 5 MJ to the inner vertical target (IVT), and

TABLE I
THERMAL SCENARIOS DEFINED BY COMPASS-U GROUP

#	scenario description	
1	Cooldown with RT vessel, transient Cryogenic cooldown (from 293 K to 80 K) with vessel on room temperature (293 K). Support structure needs to be cooled slowly (to limit thermal stresses), so cooldown should take one week. Vessel heatup with cryogenics on RT, transient Heating up vessel (from 293 K to 800 K) with cryogenics on room temperature (293 K). Cryogenics should be running (maintaining coils at 293 K actively). Vessel heatup should take approximately two days to limit thermal stresses of in-vessel components. Vessel heatup with cryogenics cooled down, transient Heating up vessel (from 293 K to 800 K) with cryogenics cooled down (80 K). Vessel heatup should take approximately two days to limit thermal stresses of in-vessel components.	done
2	Vessel bakeout without cryogenics, transient Heat up vessel from 293K to 500K (should take ~ 12 hours), keep that temperature for 24 hours and then cool down vessel back to 293 K (also ~ 12 hours).	
3	Regular tokamak full power operation - RT vessel, transient, Scenario 6408 Starting point - Cryogenics cooled down, vacuum vessel on 293 K. Shot every 30 minutes, in total 21 shots, that gives 10 hours of operation. After operation ends, "overnight cooldown" should follow - 14 hours of just cooling back to starting temperatures (both cryogenics and vacuum vessel running)	done
4	Regular tokamak full power operation - hot vessel, transient, Scenario 6408 Starting point - Cryogenics cooled down, vacuum vessel on 800 K. Shot every 30 minutes, in total 21 shots, that gives 10 hours of operation. After operation ends, "overnight cooldown" should follow - 14 hours of just cooling back to starting temperatures (both cryogenics and vacuum vessel running)	
5	Tokamak operation with limited cryogenics power - RT vessel, transient, Scenario 6408 Starting point - Cryogenics cooled down, vacuum vessel on 293 K. Shot every 60 minutes, in total 11 shots, that gives 10 hours of operation. After operation ends "overnight cooldown" should follow.	
6	Tokamak operation with limited cryogenics power - hot vessel, transient, Scenario 6408 Starting point - Cryogenics cooled down, vacuum vessel on 800 K. Shot every 60 minutes, in total 11 shots, that gives 10 hours of operation. After operation ends "overnight cooldown" should follow.	
7	Tokamak commissioning with extremely limited cryogenic power and no vessel heating systems, transient, Scenario 6408 Starting point - Cryogenics cooled down, vacuum vessel on 293 K. Shot every 6 hours, in total 3 shots, that gives 12 hours of operation. After operation ends "overnight cooldown" should follow.	
8	Cryogenics should have limited power to 100 kW.	
9	Tokamak commissioning with extremely limited cryogenic power and no vessel heating systems, transient, Scenario 6408 Starting point - Cryogenics cooled down, vacuum vessel on 293 K. Shot every 6 hours, in total 3 shots, that gives 12 hours of operation. After operation ends "overnight cooldown" should follow.	ongoing
10	Cryogenics should have limited power to 20 kW. No vessel heating/cooling!	
11	Cryostat leak, transient Starting point - cryogenics cooled down to 80 K, vacuum vessel on 800 K. At that point, introduce cryostat leak - that means thermal conductivity by convection from hot parts to cold parts. Cryogenic system and vessel heating both running. Run simulation long enough to see some equilibrium. However also first moment are important (what will be surface temperature of coils in first hours/two hours/etc?)	done
12	Failure of cryogenic system with hot vacuum vessel, transient Starting point - cryogenics cooled down to 80 K, vacuum vessel on 800 K. At that point stop cryogenic system and vessel heating system. Run simulation long enough to see some equilibrium.	
13	Failure of vacuum vessel heating with cooled support structure/coils, transient Starting point - cryogenics cooled down to 80 K, vacuum vessel on 300 K. At that point stop vessel heating system, keep cryogenics running. Run simulation long enough to see some equilibrium.	
14	Combination 10+11, transient Same as #11, but with atmosphere present in cryostat Combination 10+12, transient Same as #12, but with atmosphere present in cryostat	

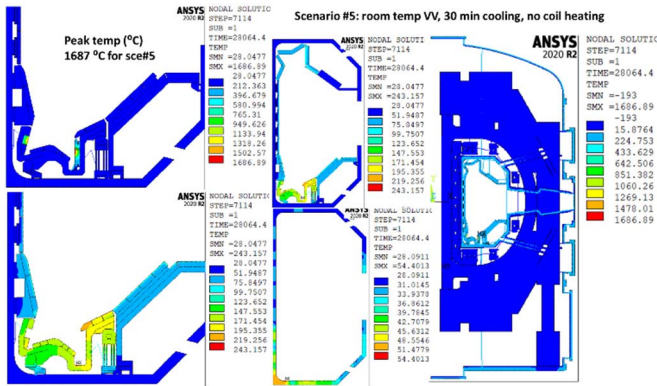


Fig. 7. Peak temperature (°C) and end-of-16th-pulse (EOP) temperature distributions.

remaining 7.5 MJ is mostly uniformly deposited to all PFCs by radiation.

Here, in this article, scenario 5 results are shown as an example, which simulates a room temperature VV with full power plasma operation full day. Fig. 7 shows the temperature distribution in the machine and peak temperature (1687 °C) in the divertors.

Fig. 8 shows the history plot of sampling points, which indicates the temperature ratcheting in the component during the repeated pulse-dwelling cycles. Also, it can be seen that some components, e.g., divertor targets OVT and IVT, reach

Temp (°C) of Inner rail (1), outer rail(2), both ends of two flex links(3-6), inner baffle(7), protection of stabilizer plate(8), HFS(9 inconel,10 tungsten), outer target(11), dome(12),and inner target(13).

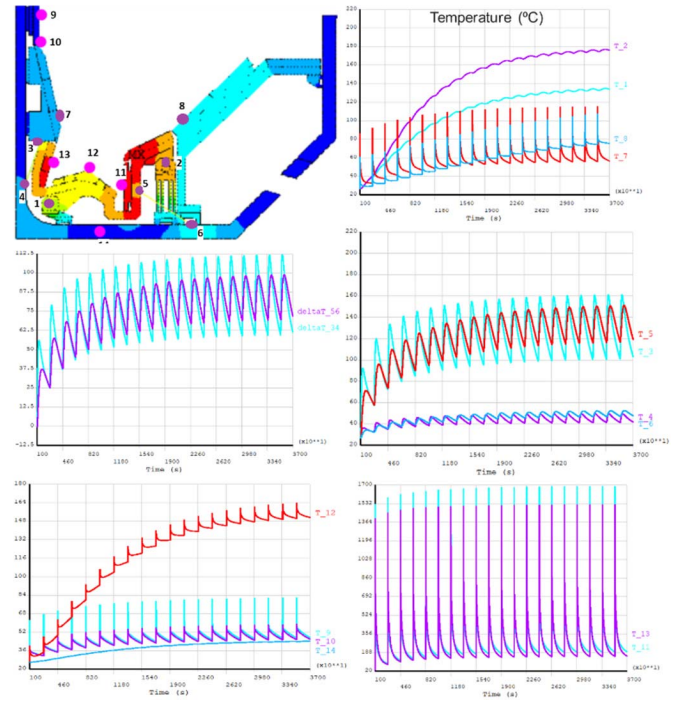


Fig. 8. History temperature plots of sampling points.

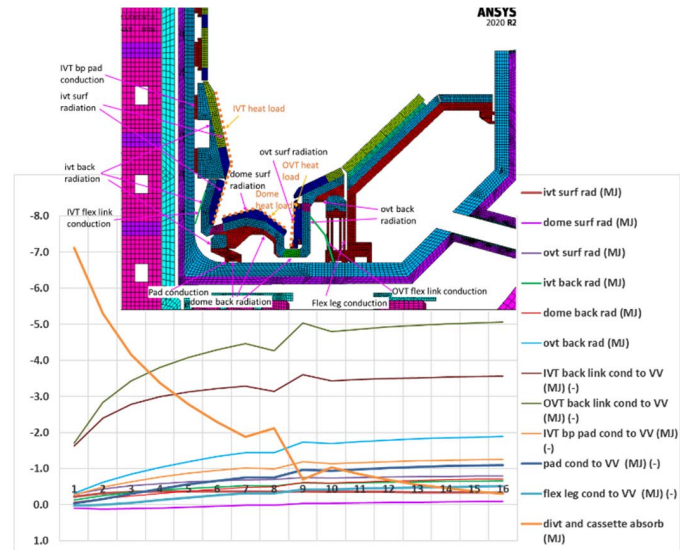


Fig. 9. Heat flow in the divertor-cassette region, by integrating power with respect to time.

their heat saturation after a few cycles, and some other component's temperature keeps rising up. If the component's thermal stress is due to peak temperature, from these plots, we can figure out the peak temperature profile, map to structural model to calculate thermal stress. If thermal stress is due to delta T within or between components, we can also use these plots to identify maximal delta T, which will be used to analyze thermal stress.

Fig. 9 shows the heat flow in the divertor-cassette region with respect to pulse-dwelling cycles. During the first few cycles (1-9), most of heat was absorbed by the thermal mass of divertor-cassette. After that, they saturate and their

TABLE II
HEAT FLOW IN THE MACHINE (AFTER 16 SHOTS)

Scenario #5	
Plasma energy (MJ)	360.0023
CS&PF energy (MJ)	0.0022
TF energy (MJ)	0.0053
CS&PF cooling (MJ)	-2.1629
TF cooling (MJ)	-8.2374
VV heating (MJ)	-165.8108
TF supt cooling (MJ)	-83.4903
CS tube cooling (MJ)	-0.8769
radiation to enviro (MJ)	24.9822
conv to enviro (MJ)	68.9805
PFC absorb (MJ)	-33.5239
Structure absorb (MJ)	-93.2312

temperatures are high, and heat was conducted and radiated to VV. To reduce the temperature gradient between the divertor and VV, flexible links made of copper, implemented by thermal link elements, are included to thermally anchor the divertor directly to the VV. The heat flow shows that the flex links at the back of IVT and OVT backplate take dominant effect after a few cycles, which indicate the significant improvement by adding these flex links.

Table II lists the heat distribution in the machine upon scenario #5 heat load after whole day operation.

- 1) Total plasma energy is $22.5 \times 16 = 360$ MJ.
- 2) Peak temperature is 1687 °C at OVT, 1550 °C at IVT, and peak EOD temperature 190 °C. Simulation of 14-h overnight cooling was done too, showing that OVT temperature will drop to ~ 70 °C. OVT, IVT, and dome cannot be fully cooled down to RT with RT helium gas cooling. A solution might be lower VV cooling inlet temperature from 27 °C to 0 °C for some time and then recover.
- 3) System has not reached steady state at the end of a day.
- 4) Cassette temperature is significantly reduced by adding the flex links.
- 5) Although cooling line design and parameters still need to be improved and calibrated at this time, comparing connecting flex links to VV and connecting flex link to cooling tube, the latter scheme will remove more heat, and thus, VV temperature will be lower.

To evaluate thermal stress, temperatures from this 2-D global model can be mapped to other 2-D/3-D structural models. Fig. 10 shows an example to map temperature to 3-D divertor-cassette assembly for further structural analysis.

Results of other scenarios are listed as follows.

Heating/Cryogenic Cooling Scenarios:

Scenario #1: After 25 h, coils can be cooled down to <100 K, and TF support temperature is 168–212 K.

Scenario #3: After 33.2 h, tile temperature will reach 740–775K (467 °C–502 °C) with helium gas inlet temperature 527 °C. Temperature gradient in VV is below targeted 40 K.

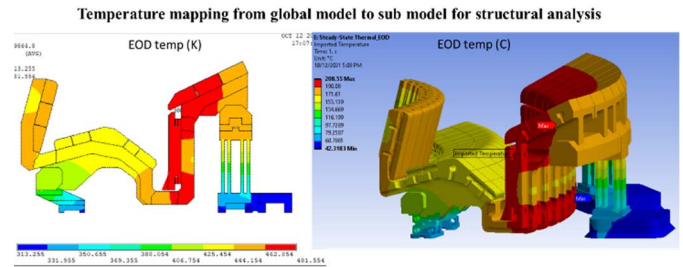


Fig. 10. Mapping temperature from 2-D global model to 3-D structural model.

Coil temperature will be from 80–91 K and TF support temperature from 136–180 K.

Normal Operation Scenarios:

Scenario #6 (500 °C VV, Cold Coil): Peak temperature 1970 °C at OVT, 1717 °C at IVT, and peak EOD temperature 527 °C.

Scenario #7: Peak temperature 1631 °C at OVT, 1259 °C at IVT, and peak EOD temperature 200 °C.

Scenario #8: Peak temperature 1938 °C at OVT, 1688 °C at IVT, and peak EOD temperature 527 °C. After 14-h overnight rest, tile temps will recover to 467°C–500 °C, coil temperatures to 80–81.5 K, and TF support temperature from 85–100 K.

Fault Scenarios:

Scenario #11: After 25.2 h, coil temperatures will be 92–110 K, no danger for the coils. VV and PFC temperature will be ~ 330 °C. Temperature of hot VV and PFC drops faster than the increase of cold mass because cryogenic components have much bigger thermal mass than hot components.

Scenario #10 is still ongoing.

IV. CONCLUSION AND DISCUSSION

A 2-D global thermal model of COMPASS-U was built and analyzed numerically with the FEA software ANSYS. Some transient simulations of different thermal scenarios were shown in this article. Results of peak temperature, temperature ratcheting profile, temperature distribution, and maximal delta T_s can be extracted and mapped to other models, either thermal submodels or structural models for further analysis. Heat flow and balance can be calculated by integrating the powers, which help to understand energy absorption and distribution, heating and cooling capacities, and thermal loading of each component.

REFERENCES

- [1] P. Vondracek et al., "Preliminary design of the COMPASS upgrade tokamak," *Fusion Eng. Des.*, vol. 169, Aug. 2021, Art. no. 112490, doi: 10.1016/J.FUSENGDES.2021.112490.
- [2] P. Titus et al., "Monitoring, modeling, and protecting against insulation failures in the NSTX-U TF outer legs," *IEEE Trans. Plasma Sci.*, vol. 47, no. 8, pp. 4165–4169, Aug. 2019, doi: 10.1109/TPS.2019.2924620.
- [3] B. Končar et al., "Thermal radiation analysis of DEMO tokamak," *Fusion Eng. Des.*, vol. 124, pp. 567–571, Mar. 2017, doi: 0.1016/J.FUSENGDES.2017.03.134.
- [4] H. Zhang et al., "NSTX-U global thermal analysis for bakeout and normal operation scenarios," *Fusion Sci. Technol.*, vol. 75, no. 8, pp. 849–861, Nov. 2019, doi: 10.1080/15361055.2019.1643687.